Low-threshold photonic-band-edge laser using iron-nail-shaped rod array

Cite as: Appl. Phys. Lett. **104**, 091120 (2014); https://doi.org/10.1063/1.4867886
Submitted: 06 January 2014 . Accepted: 23 February 2014 . Published Online: 05 March 2014

Jae-Hyuck Choi, You-Shin No, Min-Soo Hwang, Soon-Yong Kwon, Kwang-Yong Jeong, Soon-Hong Kwon, Jin-Kyu Yang, and Hong-Gyu Park

Low-threshold photonic-band-edge laser using iron-nail-shaped rod array

Jae-Hyuck Choi,[1] You-Shin No,[1] Min-Soo Hwang,[1] Soon-Yong Kwon,[2] Kwang-Yong Jeong,[1] Soon-Hong Kwon,[3] Jin-Kyu Yang,[2,a)] and Hong-Gyu Park[1,a)]
[1]*Department of Physics, Korea University, Seoul 136-701, South Korea*
[2]*Department of Optical Engineering, Kongju National University, Cheonan 330-717, South Korea*
[3]*Department of Physics, Chung-Ang University, Seoul 156-756, South Korea*

(Received 6 January 2014; accepted 23 February 2014; published online 5 March 2014)

We report the experimental demonstration of an optically pumped rod-type photonic-crystal band-edge laser. The structure consists of a 20×20 square lattice array of InGaAsP iron-nail-shaped rods. A single-mode lasing action is observed with a low threshold of $\sim 90\,\mu$W and a peak wavelength of 1451.5 nm at room temperature. Measurements of the polarization-resolved mode images and lasing wavelengths agree well with numerical simulations, which confirm that the observed lasing mode originates from the first Γ-point transverse-electric-like band-edge mode. We believe that this low-threshold band-edge laser will be useful for the practical implementation of nanolasers. © *2014 AIP Publishing LLC*. [http://dx.doi.org/10.1063/1.4867886]

Photonic crystals (PhCs) are useful platforms to manipulate photons at the wavelength scale.[1,2] In particular, PhC lasers show excellent optical properties, such as a low lasing threshold,[3–5] high Purcell factor,[6,7] and large spontaneous emission factor,[8,9] due to their high quality (Q) factors and small mode volumes. In contrast to PhC cavity lasers that confine photons in a defect region via the photonic bandgap effect, the defect-free, large-area, single-mode, PhC band-edge lasers exploit the decrease in the group velocity near the band edges in the photonic band diagram and maximize the distributed feedback effect.[10–14] Although a large output power is a primary advantage of the PhC band-edge laser, its high lasing threshold may prevent its practical implementation.

On the other hand, air-hole-type PhC slab lasers have been widely investigated thus far, in which transverse-electric-like (TE-like) resonant modes are strongly confined in a free-standing slab.[5,7,14–16] However, rod-type PhC cavities/lasers are also attractive in terms of good thermal conductivity[17] and easy current injection through the rods.[11,18,19] Moreover, such lasers can be useful for optofluidic sensing applications because of the strong interaction between the liquid used and their optical resonant modes that are sensitive to environmental changes.[11,18] Nevertheless, it is still a challenging issue to reduce the optical loss in the substrate in rod-type PhC lasers. In this work, we demonstrate a low-threshold, rod-type PhC band-edge laser by optical pumping at room temperature. The laser structure consists of a 20×20 square lattice array of iron-nail-shaped rods, in which vertical photon confinement is readily achieved in the nail heads of the rods that are fabricated using a simple but controllable wet etching process. In addition, we systematically analyze the lasing mode from measurements of the resulting spectrum and polarization state, and we compare these measurements with the numerical simulation results.

Our iron-nail-shaped PhC structure is shown in Fig. 1(a). Three pairs of InGaAsP quantum wells (QWs) with an emission peak at 1.55 μm are embedded in the nail heads of the rods as the active material (right panel, Fig. 1(a)). The InP post underneath the InGaAsP nail head has a radius R_p that is smaller than the radius of the nail head R, and thus, the resulting refractive index contrast leads to efficient vertical photon confinement in the nail heads of the rods. Emission from the QWs overlaps with a band-edge mode excited in the square lattice array of the iron-nail-shaped rods, and band-edge lasing operation is achieved. To fabricate the structure, we defined PhC patterns using electron-beam lithography and the Ar/Cl_2 dry etching process. An 800-nm-thick InP sacrificial layer was then selectively and partially wet-etched using a diluted $HCl:H_2O$ (3:1) solution (for ~1 min at 10 °C) to fabricate the post structure with its smaller radius.[5,8] Figure 1(b) shows the scanning electron microscopy (SEM) image of the fabricated PhC structure with the desired structural parameters for band-edge lasing. The rods are positioned in a 20×20 lattice, wherein the lattice constant (a) and R are 650 and 240 nm, respectively.

To theoretically investigate the optical properties of the photonic band-edge mode, the TE-like photonic band diagram was obtained using the finite-difference time-domain (FDTD) method with the periodic boundary condition in the x–y plane (Fig. 2(a)). The structural parameters used in this simulation are as follows: $R = 240$ nm, $R_p = 110$ nm, $h = 800$ nm, and $a = 650$ nm. These values are the same as the corresponding fabrication values of the device shown in Fig. 1(b). The InP post has a circular cross-section and the unit cell of the simulation is shown in the inset of Fig. 2(a). We can observe a non-degenerate band-edge mode at the first Γ-point with a normalized frequency a/λ of 0.45, which value agrees well with the peak emission wavelength of the QWs (red circle, Fig. 2(a)). This Γ-point band-edge mode is also known to exhibit highly directional emission along the vertical direction.[11–13,20] In addition, the H_z-field and electric-field intensity profiles of the first Γ-point band-edge mode were calculated for an 11×11 array of iron-nail-shaped rods using the three-dimensional (3D) FDTD method with perfectly matched layers in all boundaries (Fig. 2(b)). The field profiles are strongly confined in the nail heads of

a)Authors to whom correspondence should be addressed. Electronic addresses: jinkyuyang@kongju.ac.kr and hgpark@korea.ac.kr.

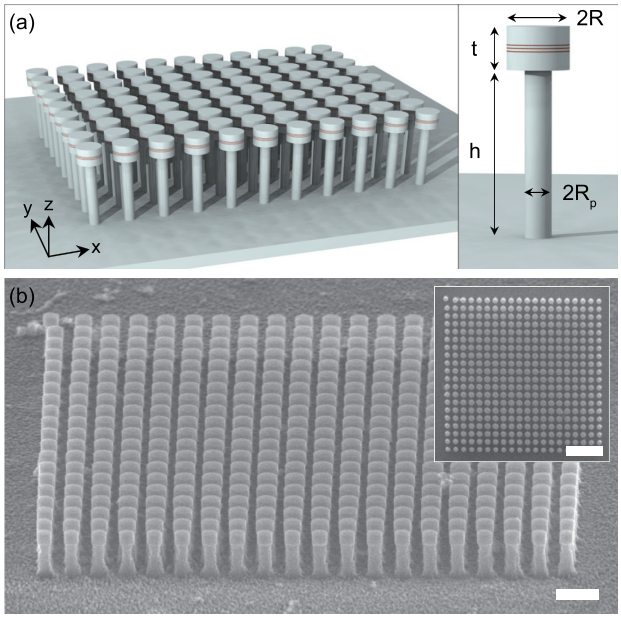

FIG. 1. (a) Schematic of photonic band-edge laser consisting of a square-lattice PhC array of iron-nail-shaped rods. In the right panel, the radius of the nail head, thickness of the nail head, radius of the post, and height of the post are indicated as R, t, R_p, and h, respectively. (b) Tilted SEM image of our fabricated structure, in which $R = 240$ nm, $t = 280$ nm, $R_p = 110$ nm, and $h = 800$ nm. The lattice constant (a) is 650 nm. The scale bar is 1 μm. Inset shows the top-view SEM image. The scale bar in the inset is 3 μm.

the rods, including the active material, as shown in the side views. From the top view, we note that the electric field intensity distribution is concentrated in each nail head, showing a central intensity minimum. Thus, a large field overlap with the active material as well as a small optical loss in the post structure are expected in this rod-type array, which can lead to desired optical properties such as a low lasing threshold.

To better understand the origin of optical loss in this PhC structure, the Q factors of the 11×11 array of the iron-nail-shaped rods were calculated as a function of the ratio of R_p and R. Figure 2(c) shows the calculated total Q (Q_{tot}), horizontal Q (Q_h), and vertical Q factors. The vertical Q factors are again divided by the Q factors Q_u and Q_d, which are related to the losses along the upward and downward directions, respectively, of the PhC structure. The simulation result shows that Q_{tot} is 3260 at $R_p/R = 0.2$, and Q_{tot} tends to decrease significantly when $R_p/R > 0.7$. Significant vertical confinement of photons in the iron-nail-shaped rods enables the achievement of a high Q factor even for the relatively large post size. In addition, the fact that Q_{tot} is numerically close to Q_h implies that the horizontal loss is more dominant. Since the finite size of the PhC array causes uncertainties in the wavevector near the band-edge point, the group velocity becomes non-zero and horizontal loss is induced.[20] With increase in the number of rods, Q_h and Q_{tot} are expected to show a corresponding increase.[21] Along the vertical direction, Q_d significantly depends on R_p/R because the downward optical loss occurs due to the presence of the post structure. On the other hand, the resonant peaks are shifted to longer wavelengths with increasing R_p/R due to increase in the modal index (right axis, Fig. 2(c)).

The fabricated structures were optically pumped at room temperature using a 980-nm pulsed laser diode (10-ns pulses

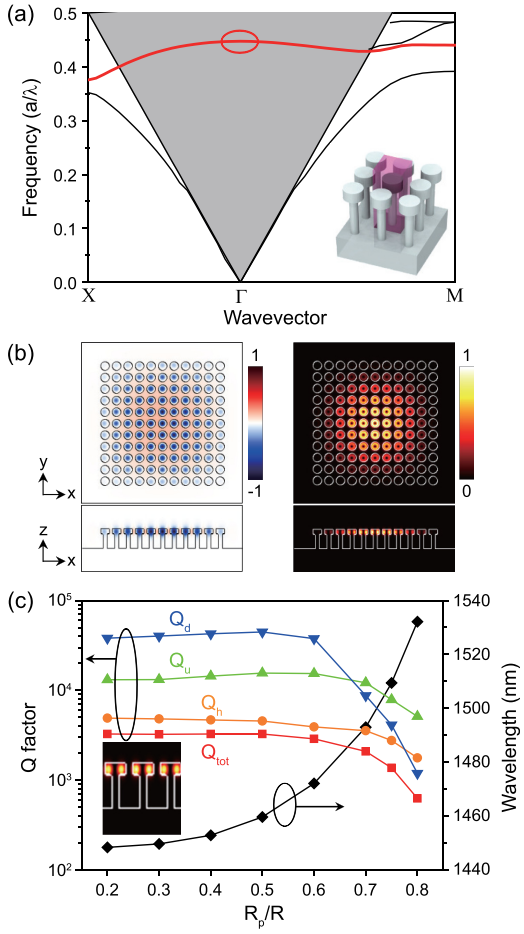

FIG. 2. (a) Calculated TE-like photonic band diagram of the square-lattice iron-nail-shaped array. The structural parameters of the device shown in Fig. 1(b) were used for the calculation. The refractive index of the iron-nail-shaped structure is set to 3.2. The red circle indicates the first Γ-point band-edge mode. Inset: unit cell of the calculation structure (purple box). (b) Calculated H_z (left panel) and $|E|^2$ (right panel) field profiles of the first Γ-point band-edge mode. An 11×11 array of the iron-nail-shaped rods was used for the calculation. (c) Calculated Q factors (Q_{tot}, Q_h, Q_u, and Q_d; left axis) and resonant wavelengths (right axis) as a function of R_p/R. The structural parameters are the same as those in (b). Inset: side-view of $|E|^2$ field profile at $R_p/R = 0.4$.

with 1% duty cycle). A 40× microscope objective lens with a numerical aperture of 0.55 was used to focus the pumping beam to a spot size of ~4 μm, and the light emitted from the structures was collected in either an infrared (IR) camera or a monochromator using the same lens. Then, strong light emission was observed in the optically pumped PhC region. A donut-shaped mode image with a size similar to that of the pumping spot was captured by the IR camera in the structure of Fig. 1(b) (inset, Fig. 3(a)). As the pump power was increased, a sharp single-mode lasing peak was observed at a wavelength of 1451.5 nm (Fig. 3(a)). To confirm lasing operation, we measured the output intensity of the peak as a function of the incident peak pump power (left axis, Fig. 3(b)). A superlinear increase in output intensity was clearly observed with a low lasing threshold of ~90 μW. It is to be noted that this lasing threshold is considerably lower than those of previously reported PhC band-edge lasers.[10,11,14] In our rod-type PhC laser, unwanted carrier diffusion over the optically pumped region was suppressed, and the structure was fabricated without damaging the active material by using only

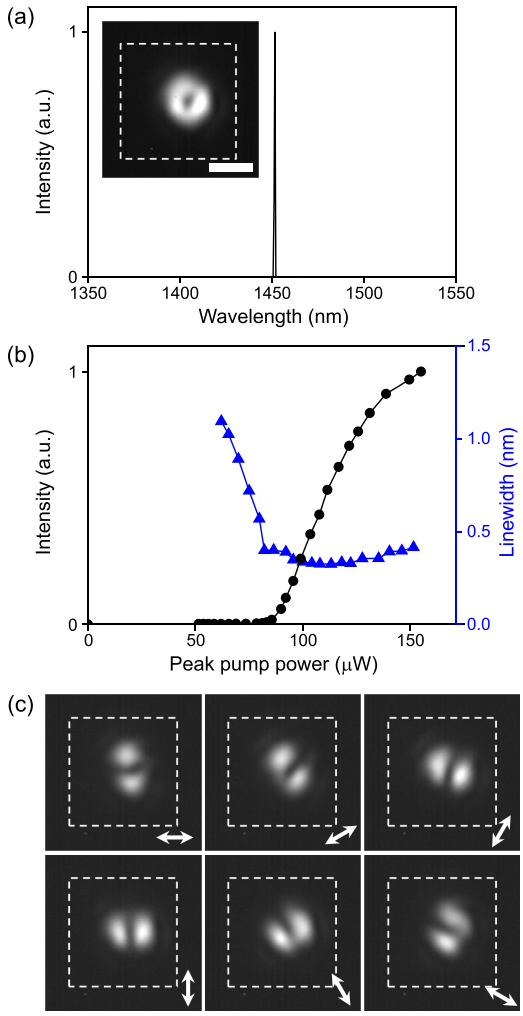

FIG. 3. (a) Above-threshold lasing spectrum and captured mode image (inset). Inset: the dotted square indicates the entire sample size, and the scale bar is 5 μm. (b) Measured lasing output intensity (black circles, left axis) and spectral linewidth (blue triangles, right axis) as a function of the incident peak pump power. The lasing threshold is ~90 μW. (c) Measured polarization-resolved lasing mode images as a function of the polarization angle.

simple fabrication procedures such as selective wet etching. The spectral linewidth of the peak was also measured (right axis, Fig. 3(b)), which showed a rapid decrease to the resolution limit of our monochromator, ~0.3 nm, soon after the lasing threshold. In addition, to investigate the polarization characteristics of the lasing mode, we positioned a linear polarizer in front of the IR camera and measured the polarization-resolved mode images as a function of the polarization angle. The observed mode images exhibit an intensity minimum along the direction of the polarizer (Fig. 3(c)), which indicates that the electric-field direction is distributed along the circumference of the donut-shaped mode.[22] Further study will be necessary to examine the thermal property of our structure and the possibility of continuous-wave (CW) lasing operation.

To clearly identify the observed lasing mode, the 3D FDTD simulations were performed. First, we calculated the field profiles of the first Γ-point band-edge mode by also considering the experimental pumping conditions. Since the lateral confinement of a band-edge mode originates from the refractive index change caused by the optical-pumping-inducing carriers, the pumping area corresponds to the lateral

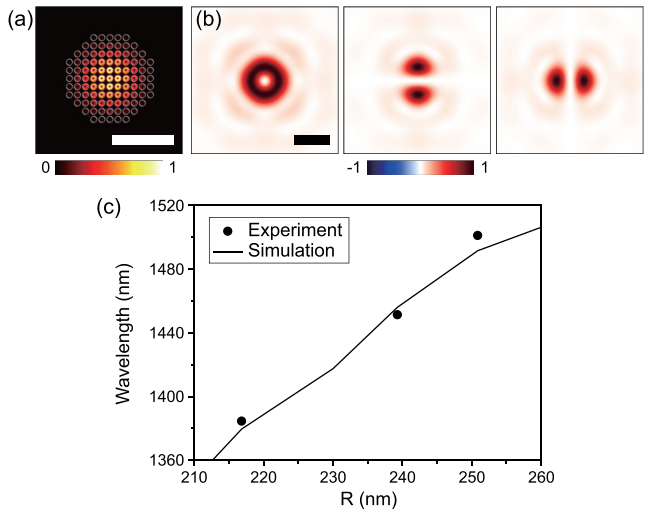

FIG. 4. (a) Calculated electric field intensity distribution of the first Γ-point band-edge mode, obtained by considering the PhC pattern within the experimental pumping area. The structural parameters are the same as those in Fig. 2(b). The scale bar is 5 μm. (b) Calculated z-components of the total (left), horizontally polarized (middle), and vertically polarized (right) time-averaged Poynting vectors at a position 14.5 μm above the PhC pattern. The scale bar is 5 μm. (c) Calculated (line) and measured (dots) resonant wavelengths plotted as a function of R. In the simulation, R_p/R was fixed at 0.46.

extension of the band-edge mode.[11] Thus, we considered only the PhC pattern within the pumping area for the simulation (Fig. 4(a)). We did not consider the effective index contrast due to optical pumping, and the simulation result could be an estimate.[11] As observed from the z-components of the total, horizontally polarized, and vertically polarized Poynting vectors at a position 14.5 μm above the PhC pattern (Fig. 4(b)), these calculated profiles closely reproduced the measured total and polarization-resolved mode images shown in Figs. 3(a) and 3(c). The mode sizes also exhibit good agreement between the simulation and experimental results. Second, we calculated the resonant wavelengths of the first Γ-point band-edge mode as a function of R, and we compared these values with the measured lasing wavelengths of the three samples (Fig. 4(c)). The band-edge laser corresponding to Fig. 3 is shown at $R = 240$ nm, and the other two laser samples ($R = 215$ and 250 nm) also exhibit identical optical properties, including the mode image and polarization state. The ratio R_p/R was fixed to 0.46 in the simulation based on the fabricated structures. We note that the calculated resonant wavelength of each mode agrees well with the measured one. The slight discrepancy between the experimental and calculated results is due to structural imperfections in fabrication. Overall, the simulation results strongly support the conclusion that the observed lasing mode originated from the first Γ-point band-edge mode.

In summary, we demonstrated an optically pumped iron-nail-shaped PhC band-edge laser with a low threshold of ~90 μW, at room temperature. The post structure of the rod, with a radius smaller than that of the nail head, was fabricated to achieve significant vertical photon confinement by using a simple but controllable wet etching process. In addition, the laser mode was identified as the surface-emitting first Γ-point band-edge mode from measurements of the polarization-resolved mode images and lasing wavelengths. Further, these measurements agreed closely with the 3D

FDTD simulation results. We expect that efficient current injection can be achieved in the iron-nail-shaped rod array through the graphene sheet covering the top surface of the nail heads.[19,23] The demonstration of this low-threshold PhC band-edge laser represents a significant step toward the practical implementation of an electrically driven, large-area surface-emitting laser that does not involve complicated fabrication procedures.

H.-G.P. acknowledges support by the National Research Foundation of Korea (NRF) grant funded by the Korean government (MSIP) (No. 2009-0081565). S.-H.K. acknowledges support by the NRF grant funded by the Korean government (MSIP) (No. 2013R1A2A2A01014491). J.-K.Y. acknowledges support by the NRF grant funded by the Korean government (MSIP) (Nos. 2013R1A1A2074801 and 2011-0015030).

[1]S. Noda, M. Fujita, and T. Asano, Nat. Photonics **1**, 449 (2007).
[2]M. Notomi, Rep. Prog. Phys. **73**, 096501 (2010).
[3]B. Ellis, M. A. Mayer, G. Shambat, T. Sarmiento, J. Harris, E. E. Haller, and J. Vučković, Nat. Photonics **5**, 297 (2011).
[4]K. Takeda, T. Sato, A. Shinya, K. Nozaki, W. Kobayashi, H. Taniyama, M. Notomi, K. Hasebe, T. Kakitsuka, and S. Matsuo, Nat. Photonics **7**, 569 (2013).
[5]K.-Y. Jeong, Y.-S. No, Y. Hwang, K. S. Kim, M.-K. Seo, H.-G. Park, and Y.-H. Lee, Nat. Commun. **4**, 2822 (2013).
[6]T. Baba, D. Sano, K. Nozaki, K. Inoshita, Y. Kuroki, and F. Koyama, Appl. Phys. Lett. **85**, 3989 (2004).
[7]Y. Zhang, M. Khan, Y. Huang, J. Ryou, P. Deotare, R. Dupuis, and M. Lončar, Appl. Phys. Lett. **97**, 051104 (2010).
[8]H.-G. Park, S.-H. Kim, S.-H. Kwon, Y.-G. Ju, J.-K. Yang, J.-H. Baek, S.-B. Kim, and Y.-H. Lee, Science **305**, 1444 (2004).
[9]S. Strauf, K. Hennessy, M. T. Rakher, Y.-S. Choi, A. Badolato, L. C. Andreani, E. L. Hu, P. M. Petroff, and D. Bouwmeester, Phys. Rev. Lett. **96**, 127404 (2006).
[10]S. Kim, S. Ahn, J. Lee, H. Jeon, P. Regreny, C. Seassal, E. Augendre, and L. D. Cioccio, Opt. Express **19**, 2105 (2011).
[11]L. Ferrier, O. El Daif, X. Letartre, P. Rojo Romeo, C. Seassal, R. Mazurczyk, and P. Viktorovitch, Opt. Express **17**, 9780 (2009).
[12]D. Ohnishi, T. Okano, M. Imada, and S. Noda, Opt. Express **12**, 1562 (2004).
[13]H. Matsubara, S. Yoshimoto, H. Saito, Y. Jianglin, Y. Tanaka, and S. Noda, Science **319**, 445 (2008).
[14]S.-H. Kwon, H.-Y. Ryu, G.-H. Kim, and Y.-H. Lee, Appl. Phys. Lett. **83**, 3870 (2003).
[15]Y.-S. No, H.-S. Ee, S.-H. Kwon, S.-K. Kim, M.-K. Seo, J.-H. Kang, Y.-H. Lee, and H.-G. Park, Opt. Express **17**, 1679 (2009).
[16]H.-S. Ee, K.-Y. Jeong, M.-K. Seo, Y.-H. Lee, and H.-G. Park, Appl. Phys. Lett. **93**, 011104 (2008).
[17]D. R. Lide, *CRC Handbook of Chemistry and Physics*, 88th ed. (CRC Press, Boca Raton, FL, 2007).
[18]T. Xu, N. Zhu, M. Y.-C. Xu, L. Wosinski, J. S. Aitchison, and H. E. Ruda, Appl. Phys. Lett. **94**, 241110 (2009).
[19]J. M. Lee, J. W. Choung, J. Yi, D. H. Lee, M. Samal, D. K. Yi, C.-H. Lee, G.-C. Yi, U. Paik, J. A. Rogers, and W. I. Park, Nano Lett. **10**, 2783 (2010).
[20]L. Ferrier, P. Rojo-Romeo, E. Drouard, X. Letatre, and P. Viktorovitch, Opt. Express **16**, 3136 (2008).
[21]H.-Y. Ryu and M. Notomi, Phys. Rev. B **68**, 045209 (2003).
[22]T.-P. Vo, A. Rahmani, A. Belarouci, C. Seassal, D. Nedeljkovic, and S. Callard, Opt. Express **18**, 26879 (2010).
[23]Y.-H. Kim, S.-H. Kwon, J. M. Lee, M.-S. Hwang, J.-H. Kang, W. I. Park, and H.-G. Park, Nat. Commun. **3**, 1123 (2012).